

# An Efficient Early-Onset Plant Disease Prediction using Improved Heuristic-aided Adaptive Ensemble Network with Leaf Image-based Phenotype Data

Thiraviam K\* & Karthiyayini R

Department of Computer Applications, University College of Engineering (BIT Campus), Anna University, Tiruchirappalli 620 024, Tamil Nadu, India

*Received 06 May 2024; revised 28 August 2024; accepted 22 January 2025*

Plant-related diseases pose a pressing threat to the agricultural industry, which is already strained to meet growing food demands. Farmers, whose primary income relies on agricultural production, often confront significant challenges as these diseases can severely disrupt crop growth and quality. Without early prediction, such diseases can greatly reduce crop productivity. Hence, to overcome this threat at an early stage, this research concentrates on developing an effective Adaptive Ensemble Network with a novel loss and activation function model for early-onset plant disease prediction using plant leaf imagery. In this method, the vital features are extracted from the Residual Network (ResNet152), Visual Geometry Group (VGG19), and DenseNet161. After attaining the features, the final feature set is obtained by the averaging-based computation. Then, the resultant features are given to the Deep Temporal Convolution Network (DTCN) for prediction of early-onset plant disease, in which the loss and activation functions are newly derived. Furthermore, parameter tuning uses the Modified Update in the Coati Optimization Algorithm (MUCOA). Finally, the validation outcomes of the designed approach are validated against conventional frameworks. The suggested framework performs robustly, achieving maximum accuracy, sensitivity, and specificity values exceeding 93% across both datasets. As a result, the proposed AEN model can be an insightful, farmer-friendly aid in identifying and predicting the early beginnings of plant leaf diseases.

**Keywords:** Adaptive ensemble network, Early-onset plant disease prediction, Feature extraction, Leaf phenotype data, Novel loss and activation function

## Introduction

The term agriculture played a crucial role in the economy.<sup>1</sup> Over the last decades, agriculture acquired the dominant position because of diverse factors like climatic conditions, environment, and social and political reasons, its productivity has declined.<sup>2</sup> In addition, plant disease acquired a catastrophic influence on the production of agriculture as well as posed a severe threat to the security and protection of food globally.<sup>3</sup> Moreover, the traditional techniques for detecting infection in plants require the knowledge of professionals and a great deal of expertise.<sup>4</sup> Thus, the control of plant disease and diagnosis was most significant for ensuring maximized production. Consequently, image-dependent phenotyping techniques provided a wide range of advancement.<sup>5</sup> Concerning long experiments, they were usually non-destructive, where the phenotypic data had been aggregated through the same organism.<sup>6</sup> More specifically, plant phenotyping is a technology and

information-dependent domain along with specified limitations and domains for detecting and diagnosing plant disease.<sup>7</sup> To alleviate these issues, it is significant to retrieve adequate information from the images and further concentrate on phenotyping traits like tomato stem nodes, flowers, and fruits as well as monitoring them at the time of plant growth.<sup>8</sup> Thus, this information was aided in offering an assessment of the plants' quality constantly and it maximized the entire production.<sup>9</sup>

Commonly, the plants affected by the disease had phenotypically varied through healthy ones in pattern, colour, and shape.<sup>10</sup> Thus, the question of how to maximize the production of fruits has been considered as a major issue in digital agriculture. Moreover, certain crops were propagated with issues like shading thus resulting in irrelevant quality of fruit.<sup>11</sup> Further, it was also important to derive the difference between the ripe and unripe fruits. More research work has determined that automated plant disease detection depending on machine learning techniques and image processing has maximized the speed and accuracy of diagnostic outcomes.<sup>12</sup> More specifically, advanced

\* Author for Correspondence  
E-mail: akthiraviam@gmail.com

approaches like digital image processing techniques as well as the Principle component analysis techniques were utilized to diagnose diverse crop diseases. Along with the maximized open-source datasets, diverse crop diagnostics validations like grape, apple, and paddy have attained an average accuracy.<sup>13</sup>

In general, machine intelligence-dependent techniques such as deep learning, machine learning as well as the usage of computer vision with the IoT equipment help the farmers and thus make the process of farming easier.<sup>14,15</sup> Deep learning techniques possess diverse advantages over machine learning techniques, and their strategies have been used in diverse applications for the past few years.<sup>16</sup> Consequently, machine learning approaches like k-Nearest Neighbors (k-NN) and Artificial Neural Networks (ANN) have restricted trials on the detection of plant disease out coming in a minimized rate of accuracy and thus leading to the temporal validations of disease conditions<sup>17</sup> at the same time these approaches faced various limitations in the plant disease detection. Thus, the phenotype information had been acquired for significant diagnosis of the plant disease using recent methodologies. Thus, a new earlier onset disease prediction model was implemented in this work. This paper presented a deep learning approach based on plant disease prediction, which can predict multiple diseases on plants based on the phenotype images. The early-onset prediction of disease minimizes the cause of heavy damage to the crop, which helps to increase the economy and productivity of plants. It is necessary to take effective and efficient control against the disease for the support of sustainable development. Identifying the disease is important to analyze the reason for the disease and take control measures that will save time and cost. The framework of the model offers better effective and significant method for practical applications.

The main contribution of the model is provided as follows.

- To design the Adaptive Ensemble Network (AEN) model that comprises ResNet152, VGG19, and DenseNet161 for retrieving the most significant features, and the average computation-based resultant features are fed into the DTCN for the early onset prediction of plant leaf diseases by utilizing image-dependent phenotype data with the aid of loss and active functions.
- To develop the MUCOA algorithm derived from the conventional COA, which is used to perform parameter optimization to maximize the performance of the AEN approach.
- To perform the analysis in the developed model via diverse measures to confirm its performance.

## Literature Survey

### Related Works

Cardellicchio *et al.*<sup>18</sup> have intended to detect the phenotyping traits on the tomato plant by utilizing the single-phase detectors depending using YOLOv5 that focused on significantly detecting the nodes, flowers, and fruits over the difficult datasets that were taken at the time of validation. The outcomes from the model have shown that it has attained a high score concerning all the difficulties in terms of colour, similarity among the objects as well as object size. Bhatia *et al.*<sup>19</sup> have suggested a new approach called as Fractional Mega-Trend Diffusion (FMTD), which was a feature extraction method that contributed to the speed and accurate detection of disease over the plants. Further, the feature extraction approach was proposed to extend the small dataset into maximized feature space by validating the new features with the aid of FMTD functions. For the datasets, the resembling approach has been implemented and the Optimized Kernel Extreme Learning Machine (OKELM) algorithm model was utilized to perform the categorization process. Thus, the resultant outcomes have shown the enriched performance of the framework.

Arshad *et al.*<sup>20</sup> have implemented a new hybrid-based deep learning technique to automatically identify the disease over potato leaves. Further, it has employed ensemble techniques by integrating the deep features through standard techniques VGG19 and Inception-V3 to attain the relevant features. For acquiring the final predicted outcomes, the hybrid techniques leveraged the concept of a vision transformer. Thus, the investigational findings have confirmed that the model provides accurate and effective detection outcomes and it has been used for practical applications. Yang *et al.*<sup>21</sup> have recommended the new Triple-Branch Swin Transformer Classification (TSTC) network that has been utilized for the categorization of plant disease. In the initial phase, the preliminary features were retrieved with the help of a triple-branch network that was developed depending on the ST. Then, the

compact bilinear pooling approach was used for fusing the features to improve the learning ability of the feature extractor, and thus more discriminative features were retrieved. In the end, the deep supervision module has integrated losses, so that it has trained in the directions, where all the layers have been effectively working for severity and disease classifications.

Dahiya *et al.*<sup>22</sup> have validated diverse deep learning architectures, in which it has been tested for identifying plant disease. For this validation, the MATLAB R2019b was used. In the end, the accuracy of the deep learning techniques has also been calculated. Bhakta *et al.*<sup>23</sup> have suggested a model depending on the thermal images by determining the dynamic features of deep learning techniques. The designed techniques have included the three convolutional layers for tackling the over-fitting and computational issues. The system was tested along with diverse common diseases.

Chug *et al.*<sup>24</sup> have developed a new model for optimizing the hyperparameters, the Optuna framework was utilized in this work. Then, the validation of this model was made using two plant disease-related datasets. Thus, this model has aided the farmer to minimize the workload that permitted them to treat the disease in the earlier phase. Ramanadham & Savarimuthu<sup>25</sup> have presented the new model represented as a Deep Ensemble Neural Network (D-ENN) approach to automatically detect plant disease. Thus, the D-ENN model was regarded as an effective tool for agronomists and farmers for

quantifying and diagnosing cotton diseases. Enormous studies related to the plant leaf disease prediction and its merits and demerits are given in Table 1.

### Methodology of Proposed AEN for Predicting the Early Onset of Plant Leaf Disease

#### Proposed AEN Model

In the AEN, the ensemble is the process of combining the two more deep learning models to ensure better feature representation and prediction. The adaptive concept is more efficient than the standard models. The function of the adaptive concept is used to optimally tune the parameters for improving the efficiency of the task. It enhances the sustainability and accuracy. The combination of adaptive ensemble networks enhances the robustness and provides accurate output. In our proposed methodology, ResNet152, VGG19, and DenseNet161 are the techniques taken for predicting the disease. The three different models utilized in this research for detecting plant disease and this model are executed in a parallel way that can be used to lower the computation power and reduce the overall time for the execution process. Additionally, the parameters of the three different models are optimized to reduce the overall computational load, thereby enhancing efficiency and expediting processing. Initially, these three networks are employed for retrieving the essential features using the layers present in the network. Further, these features are concatenated by computing their average value. The consequential features are then input to the

Table 1 — Certain features and limitations of the conventional disease prediction over plant leaf imagery

Methodology	Advancements	Limitations
YOLOv5 <sup>(18)</sup>	It effectively detects the abnormality region with the help of a boundary box that helps to significantly identify the diseases.	It only handles a single type of plant leaves. It is further applied for the collection of multiple plant leaves.
FMTD <sup>19</sup>	It achieves superior results by considering the tuned parameters for the classifier model.	Since it manages the two different datasets, it can cause the computation as well as time complexity.
PLDPNet <sup>20</sup>	It provides better feature representation and it employs the transformer network to present better classification results.	The ensemble-based feature process can produce a dimensionality problem that can mislead the mechanism.
TSTC <sup>21</sup>	It obtains a more accurate value for disease identification as well as severity classification.	Over fitting issues can occur as they involve multiple layers along with the transformer network.
CNN <sup>22</sup>	It utilizes such an optimizer for computing the optimized values.	Over fitting issues might degrade the system's efficiency.
VGG16 and VGG19 <sup>(23)</sup>	It yields the dynamic values of features and it also evades the computation and over fitting problem.	It does not support real-time databases and leaf images.
Efficient Net, KNN, RF <sup>24</sup>	It estimates the high positive rate and less negative rate while classifying the plant diseases.	It does not have the potential to tackle the massive collection of images.
D-ENN <sup>25</sup>	It can deduce the ensemble and detection loss and it attains impressive results.	It does not take the pathological parameters for diagnosing the diseases.

DTCN framework, which performs the prediction. To enhance the model's efficiency, the parameters in the ensemble framework were optimized using the developed MUCOA.

**Recommended Method of Predicting the Early Onset Prediction of Plant Disease**

In modern times, the agricultural sectors have faced various issues in identifying and detecting plant diseases. Some traditional techniques used for the prediction process rely on crop inspections by agronomists to detect indicator signs. Additionally, plant and crop diseases have led to significant losses in food production and security. In recent years, climatic changes and global trade have exacerbated the conventional conditions of plant diseases, impacting the new challenges agriculture faces. To alleviate these challenges, numerous studies have been conducted to mitigate the impact of environmental and weather conditions on major food crops. To enhance the processes of crop management and plant health, various research avenues have been explored for the early prediction of diseases, although adverse stresses persist. Furthermore, image-based methods can depict non-invasive and autonomous techniques for predicting plant diseases. The validation of images has revealed a host of computational approaches with the potential to retrieve information through digital images. However, the automatic processing of acquired images to provide desired measurement datasets is yet to be fully developed. Considering the aforementioned points, this research presents a new model designed to

offer better outcomes, and its architecture is provided in Fig. 1.

In this paper, the effective model of plant disease prediction by utilizing the phenotype data is considered. By using the online available standard web sources, the raw plant leaf objects are acquired in the initial stage. Then, the process of prediction has been carried out, where the AEN along with the loss and activation function has been designed. In this framework, the most relevant features have been retrieved through ResNet152, VGG19, and DenseNet161. Here, a limited amount of images is enough for training the model as we utilize the ensemble model that consists of three deep learning techniques that can provide the generalizable solution even if it is trained on a small dataset. The prediction accuracy is greatly increased with the help of AEN because the proposed approach combines multiple deep learning techniques and provides robust outcomes in plant leaf disease prediction. The features from the three deep learning models are more helpful in predicting the disease in the plant. Most importantly, the ResNet152, VGG19, and DenseNet161 models incorporated into the AEN model analyze the color and texture of the affected area to extract the features. After obtaining the features from the AEN techniques, the unified set of features has been acquired through averaging-based computation. In the end, the resultant features have been fed to the DTCN model for predicting the disease, where it has undergone both loss and activation functions that are newly derived. The

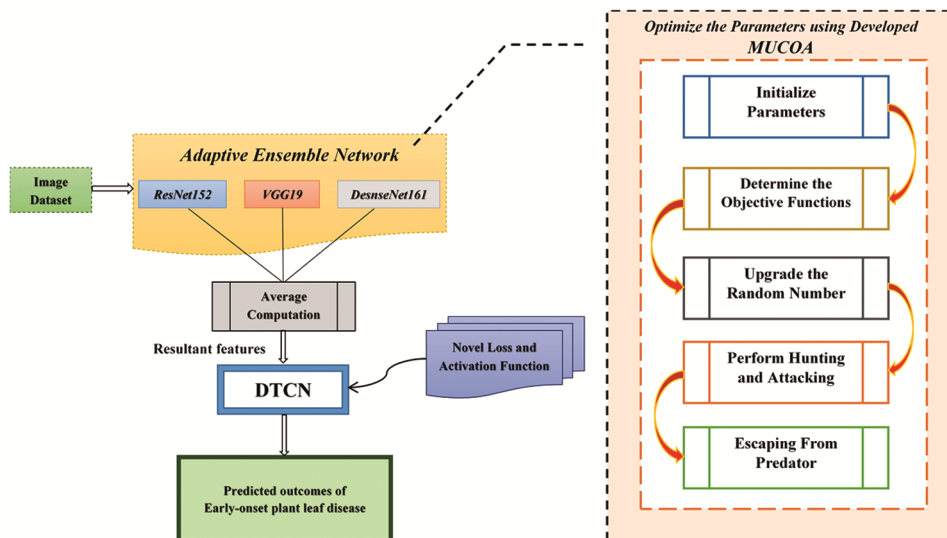


Fig. 1 —The early-onset plant leaf disease prediction model-Architecture

combined features representation is given to the DTCN along with novel loss function and activation function for predicting the plant disease. From the combined features representation, the temporal features are extracted by the temporal convolution layers. Further, the dimensions of the temporal features are reduced by the pooling layers. Based on the extracted features, the final fully connected layer predicts the disease in the plant. The addition of a novel loss function with the DTCN model helps to capture the specific characteristics in the input features and it enhances the capability of the DTCN model to get accurate results. Additionally, the novel loss functions with the DTCN ignore the irrelevant features and focus on the most important features to get accurate results in the disease prediction process. Likewise, the integration of the activation function helps the DTCN to learn the complex features that are particularly important for the disease prediction process. Moreover, in this work, for tuning certain parameters, the MUCOA has been used. Finally, the results attained from the experimentation process illustrate that the newly designed model has shown impressive outcomes in forecasting plant disease at earlier phases.

#### Modified Update in COA

For designing the earlier onset plant disease prediction framework, the modified MUCOA algorithm is designed. The major intent of designing the algorithm model is to tune the parameters that help to enhance the performance. Here, the new formulation is derived to carry out the process by tackling the limitations in the traditional COA<sup>26</sup> model. The MUCOA is mainly used for tuning the hidden neurons and epochs of the feature extraction models to improve the precision and accuracy values. The MUCOA is designed by improving the random number in the conventional COA to get the optimal and most effective solution. The new random number is calculated based on the worst and the best fitness values and it is mathematically derived in Eq. (1). The upgraded random number in the MUCOA helps to identify the solution in the new search space. The searching capability of the MUCOA helps to avoid the local optimal condition. The multi-objective problems in the search space are handled by the MUCOA and it has rapid convergence capability rather than the conventional algorithms. Specifically, the parameter tuning in the MUCOA is used to enhance the robustness of the feature extraction process. Moreover,

the interpretability of the deep learning model utilized for the feature extraction is enhanced because of the parameter optimization using the MUCOA. Along with its uses, the MUCOA reduces the training time which helps to get accurate results.

The conventional COA model has attained the optimal values in a better manner. It has the potential to offer the most adequate solutions for optimization issues by striking the relevant balance between exploration and exploitation in the global search and local search. But, there is a requirement for binary and multi-modal versions of COA.

Thus, the new derivation for random numbers has been designed in this model. It is derived in Eq. (1).

$$rd = \frac{((Ft_{bst} * 1.5) / Ft_{wst})}{N_p} \quad \dots (1)$$

Here, the number of population is given as  $N_p$ , the best and worst fitness functions are termed as  $Ft_{bst}$  and  $Ft_{wst}$ , the random function is depicted as  $rd$  and this random number if applied in the Eq. (2) of the COA.

$$A_b = a_{b,c} + rd.(UB_c - LB_c), b = 1, 2, \dots, B, \quad c = 1, 2, \dots, d \quad \dots (2)$$

The random real number derived in Eq. (1) is termed as  $rd$ , the upper and lower bounds on the  $c^{th}$  decision variables are depicted as  $UB_c$  and  $LB_c$ , the number of coatis is indicated as  $B$ , the number of decision variables is represented as  $d$ , the value of  $c^{th}$  decision variable is depicted as  $a_{b,c}$  and the location of  $b^{th}$  coati on the searching space is given as  $A_b$ . The pseudo-code for the newly designed MUCOA model is given in Table 2.

Table 2 — Pseudocode of the developed MUCOA

#### Algorithm 1: MUCOA

1. Information on optimization issues is considered as input.
2. Parameters are set
3. Initial parameters are created and the objective function is determined.
4. The position of iguana is updated.
5. if  $b > \frac{B}{2}$  then
6. Compute the random number using Eq. (2)
7. Generate the iguana position based on the upgraded random number.
8. End if
9. Save the best candidate solution
10. End

## Implementation Details of Proposed Adaptive Ensemble Network

### Dataset Details

To perform early-onset plant disease prediction, two datasets are utilized in this study, as detailed below:

*Dataset 1:* This dataset is obtained from "https://data.mendeley.com/datasets/tywbtsjrjv/1 (03 October 2024)". It contains 61,486 images across 39 distinct classes of plant leaf images.

*Dataset 2:* The comprehensive benchmark plant leaf imagery dataset, obtained from "https://github.com/liuxindazz/PDD271?tab=readme-ov-file (03 October

2024)", comprises 220,592 images distributed across various disease categories. This dataset includes images with varied symptoms and complex backgrounds of plant leaves, enhancing early prediction capabilities.

The images sourced from these datasets, termed as  $DT_l^p$ ,  $l = 1, 2, \dots, L$ , are utilized in subsequent stages of processing within the proposed framework. Sample images that illustrate the diversity of plant types across the datasets are shown in Figs 2 & 3.

### Feature Extraction

The images  $DT_l^p$  acquired during the initial phase of the proposed prediction model, are used as input to this process.

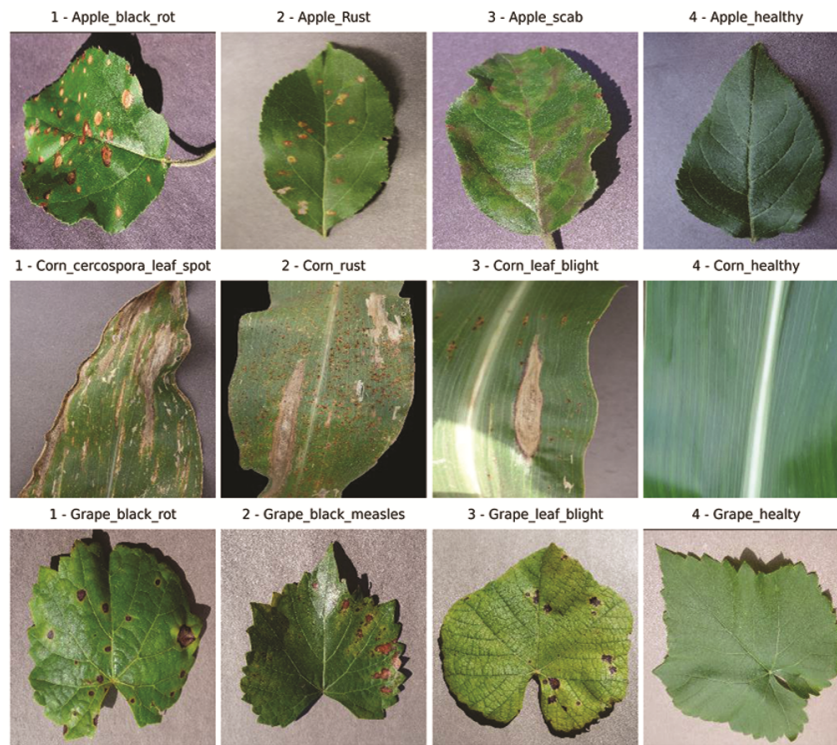


Fig. 2 — Depiction of certain sample images of Dataset 1

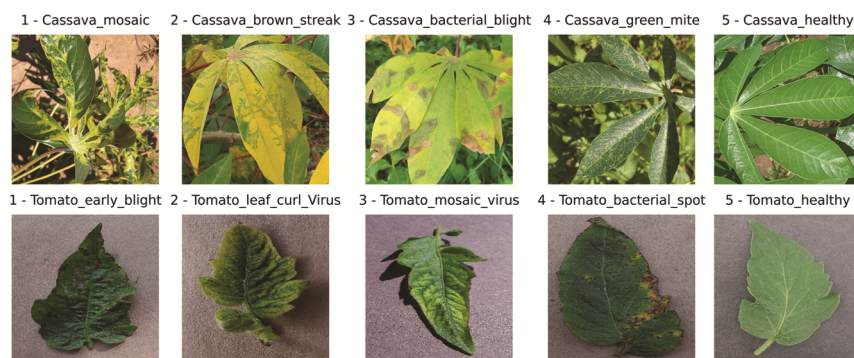


Fig. 3 — Depiction of certain sample images of Dataset 2

ResNet152<sup>(27)</sup>: The ResNet152 consists of 152 layers. The deep nature of the ResNet152 helps to analyze the intricate pattern in the leaf images to get accurate results. Further, the occurrence of vanishing gradient issues is effectively solved by the residual learning adopted in this structure. All types of images collected under various scenarios are effectively handled by the ResNet152 and the generalization capability of the model is very high. The conventional neural networking model has faced some difficulty while maximizing the depth of the network and thus the neural network has been converged. Then, it has been minimized rapidly, where the issues degrade the network performance. In this case, the ResNet152 is built with 152 convolutional layers, in which each layer is processed with stride and  $3 \times 3$  matrix of input concerning three directional ways. In addition to that, the residual map has been reconstructed depending upon the residual units and then the features have been determined utilizing diverse activation functions and convolution kernels. Further, the performance of the networking model accuracy has been maximized gradually to its critical points. Thus, it has determined the connection among the current layers and upper layer features in skip connection format. Thus, the term  $FS^{rsn}$  depicts the features attained through the ResNet152 model.

VGG19<sup>(28)</sup>: The VGG19 is made up of a series of convolution and fully connected layers. Further, the hierarchical representation of the input images is 19 layers and these layers are enough for analyzing the feature representation of the images. The fine-grained features of the images are also captured by the VGG19 architecture as these features are utilized for determining the small and the subtle variation in the images. As the name implies, this network contains 19 layers total, where it is named as 1 softmax layer, 5 max-pooling layers, 3 FC layers, and 16 convolutional layers. Rather than other models, the VGG19 is a simpler method to process with  $3 \times 3$  convolution layers to learn the features. The expression of every convolution layer is given in Eq. (3).

$$X_a^b = \phi \left( \sum_{c=1}^{N^{b-1}} X_c^{b-1} \times u_{ca}^b + v_a^{b-1} \right) \dots (3)$$

In the above equation, the convolution function describes the connection between  $c^{th}$  and  $a^{th}$  features of  $(b-1)$  layer,  $b^{th}$  layer. Further, the bias value and activation function are indicated as  $v_a$  and  $\phi$ ,

respectively. Thus, the term  $FS^{vg19}$  depicts the features attained through the VGG19 model.

DenseNet161<sup>(29)</sup>: The DenseNet161 requires a very minimum number of parameters for the process of feature extraction. The dense connection in the approach helps to discover the complex features of the plant images within a limited period. In addition, gradient flow within the DenseNet161 is better than the other models so the chance of overfitting is greatly prevented. Both high and low-level features in the images are captured in the DenseNet161 model because it consists of a dense connection and convolution layer which helps to retrieve the rich feature representation from the images. This model is an extended version of basic DenseNet. In general, the DenseNet has included the dense blocks as well as the transition blocks. Concerning the dense blocks, all the layers in these blocks are densely connected with each other. Further, the layers in the DenseNet have attained the input through output feature maps of the previous layer. When there are L layers over the networking model, then the DenseNet has acquired  $L(L + 1)/2$  connections that have typical network L with connection L.

DenseNet161 utilizes dense connectivity, a skip connection, where every layer is associated with the following levels of the network that aid in solving the gradient vanishing issue. Due to such a connection, features are effectively re-used and parameters are simplified. The feature dimension is decreased by the transition layer that is followed by four dense blocks with (6, 12, 16, 24) sub-blocks. Every sub-block encompasses two convolution layers that contain a total of 156 layers in dense block. Once the input image is given, the feature maps are generated in the first dense block, which is fed into the subsequent dense block and transition layer. At the end of the final block, the essential features are acquired and represented as  $FS^{dn}$ .

#### Average Computation

The process of combining different features from the three deep learning techniques ResNet152, VGG19 and DenseNet161 for developing a single or unified representation is called as feature averaging process which simplifies the training process.

Thus, the features attained from ResNet152, VGG19, and DenseNet161 are termed as  $FS^{rsn}$ ,  $FS^{vg19}$  and  $FS^{dn}$  accordingly. Here, the average-based computations are carried out to attain the final resultant feature. Thus, it is derived in Eq. (4).

$$RF_m^{rvd} = \frac{\{FS^{rsn} + FS^{vg19} + FS^{dn}\}}{3} \dots (4)$$

Term  $RF_m^{rvd}$  depicts the resultant features attained from the AEN model, where  $m = 1, 2, \dots, M$  denotes the total number of features. Further, the final attained fused features  $RF_m^{rvd}$  from three standard techniques are provided as the input to the DTCN model to perform the final prediction outcomes.

**DTCN with Novel Loss and Activation Function**

The feature learning capacity of the DTCN<sup>30</sup> model is very high at the same time it requires a minimum period for training the model. Further, the different type of plant disease is accurately detected by the DTCN. The complex feature in the given input information is learned by the deep convolution layer of the DTCN. Additionally, the difference between the healthy and unhealthy plant images is also determined by the DTCN model. The above reason motivated us to adopt the DTCN model for the proposed framework.

*1D Convolution:* TCN has utilized the causal convolution, in which the output at the time  $ti$  has convolved along with the elements through time  $ti$ . Further, the causal convolution has been utilized to assume that all the data has a causal relationship over the chronological order. While concerning the input sequence  $D = (d_1, d_2, d_3, d_4, d_5)$  as a time series signal along with  $d_{ii} \in \mathfrak{R}^m$  where the variable dimension is given as  $nn$ , consequently, it does not have strict causality over the chronological order. Here,  $d_1$  and  $d_5$  has the direct connection and the causal convolution has made the relationship among  $d_1$  and  $d_5$  that are affected through  $d_2, d_3, d_4$ .

*Dilated Convolution:* Dilated convolutions have been utilized in this model for enhancing the detection performance. Moreover, conventional operation techniques have been utilized to convolute the sequence. Then, pooling is performed to minimize the sequence amount as well as then enlarge the receptive field. One of the significant faults is that certain relevant information, which has been lost at the time of pooling; it has the advancement of dilated convolutions and then gradually increases the perception field. Further, dilated convolution has been employed over the issues of long information dependence of sequences like

environment forecasting, signal and voice processing, and so on. Then, the dilated convolution has been given in the Eq. (5).

$$FS(pd) = (d * dif)(pd) = \sum_{f=0}^{g-1} dif(f)h_{pd-di.f} \dots (5)$$

The filter is given as  $dif : \{0, \dots, g-1\} \rightarrow \mathbb{N}$ , the direction of the past is denoted as  $pd - di.f$ , the filter size is termed as  $g$ , and the dilation factor is given as  $dif$ .

*Residual Block:* A structure has been developed through the sequential as well as multilayer residual network and then parallel to that of residual blocks. Moreover, the basis of the residual block has been utilized in the TCN networking model however, the jump connection over the ResNet model has resulted in a lesser residual block number that have the potential to learn useful information and thus failed to adapt the time series prediction on the residual block structure.

The two channels are considered, each of the channels has nonlinearity as well as dilated convolution and they are utilized for ReLU. The same input along with two diverse convolutions are added to attain the outcomes. Moreover, the convolution layer includes kernels in multiple layers with diverse sizes. The  $g$  filter is swept by input data  $D$  and it is derived in Eqs (6 – 9).

$$ReLU(d) = \max(0, d) \dots (6)$$

$$i_{1g} = ReLU(wt_g * D + bi_g) \dots (7)$$

$$i_{2g} = ReLU(wt_g * D + bi_g) \dots (8)$$

$$i_g = i_{1g} + i_{2g} \dots (9)$$

The result of channel 1, and channel 2 are given as  $i_{1g}$  and  $i_{2g}$ , the result of the unit is depicted as  $i_g$ , and the convolution operation is termed as  $*$ . A residual block has included the channels that are propagated by  $\mathfrak{I}$  as series of conversion functions and the final output has been added up with the input  $D$  of the block is derived in Eq. (10).

$$D = (d + \mathfrak{I}(d)) \dots (10)$$

*Fully Connected Layer:* It has been replaced through Global Average Pooling (GAP) for better accuracy and efficiency over image identification tasks. Moreover, this layer is more significant for performing the prediction tasks. Then, the statistic  $j \in \mathfrak{R}^z$  has been

produced through shrinking  $D$  and its spatial dimension  $Z * Y$ , where the output  $j$  is derived using Eq. (11).

$$j = gap(d_{zz}) = \frac{1}{Z * Y} \sum_{f=1}^Z \sum_{k=1}^Y d_{zz}(f, k) \quad \dots (11)$$

The whole spatial features over the channel have been averaged as the global features.

*Novel Loss Function and Activation Function:* The AEN model is effectively performed by the integration of the novel loss function with the activation function. The difference between the predicted and actual outcome is determined. The training of the DTCN approach is guided by the novel loss function and it helps to reduce the error during the prediction of plant disease. Similarly, the addition of an activation function on the different layers of the DTCN model enhances the learning capability which helps to analyze the complex features. Further, the nonlinear relationship between the features is precisely learned by the addition of the activation function. The integration of novel loss function and activation function maximizes the predictive capability which helps to enhance the accuracy and precision values. In this work, the novel loss and active function have been designed as well as it is considered as the major attribution. The description of the loss and activation functions is detailed as follows.

*Huber Loss:* It is the integration of MSE and MAE. Thus, it has acquired the better adequate properties of loss functions through differentiable at minima. When the error is maximized, and then the Huber loss is performed or else the error is small, then the MSE part of the Huber loss is utilized.

$$loss = \begin{cases} \frac{1}{2} * (o - p)^2 & \text{if } (|o - p| \leq \tau) \\ \tau * |o - p| - \frac{1}{2} * \tau^2 & \text{otherwise} \end{cases} \quad \dots (12)$$

*Cross-entropy Loss:* It is commonly utilized for performing the classification. It is also known as the negative log-likelihood.

$$CEL = -(p_q \log(\hat{p}_q) + (1 - p_q) \log(1 - \hat{p}_q)) \quad \dots (13)$$

*Sigmoid:* Here, the sigmoid function has been typically deployed to the output nodes of categorization and thus it has resulted in either 0 or 1.

$$A = \frac{1}{(1 + e^{-x})} \quad \dots (14)$$

*Tanh Function:* This activation function outperformed consistently over the sigmoid function, and it is termed a tangent hyperbolic function.

$$f(w) = \tanh(w) = \frac{2}{(1 + e^{-2w})} - 1 \quad \dots (15)$$

**The Functionality of Proposed AEN-MUCOA Model**

The input image is fed into the ResNet 152, VGG19, and DenseNet161 for extracting the features separately. After that, these features are combined by using the average computation. The average between the elements of the feature from each model is calculated to get the final feature representation. Further, these features are given to DTCN for providing the predicted outcome, in which the loss and activation function are derived in a novel manner. The proposed AEN-MUCOA for disease prediction is displayed in Fig. 4

**Objective Function**

For performance enhancement, certain parameters are tuned using the MUCOA algorithm model. Thus, the conventional model has both advancement and limitations. So it is necessary to tackle those restrictions by deriving the new formulation.

*ResNet152:* It has attained better performance over the benchmark dataset and ensures better gradient flow and optimization. But, it has faced a lack of interpretability and complexity.

*VGG19:* In general, this model can attain a better accuracy. But, it needs more duration to train the approach.

*DenseNet161:* It can alleviate over fitting by minimizing the number of parameters. But, this model has utilized a lot of memory space.

*DTCN:* This model has the potential to adapt diverse domains and also has better control for memory size. However, it is too expensive to train the model. To tackle the disadvantages, the new derivation is formulated and it is given in Eq. (16).

$$FT = \underset{\{ep_{rn}, hn_{rn}, ep_{vg}, hn_{vg}, ep_{dn}, hn_{dn}, ep_{dtn}, hn_{dtn}\}}{\text{arg min}} \left( \frac{1}{(acc + prn)} \right) \dots (16)$$

Here, the rate of the epoch of ResNet152, VGG19, DenseNet161, and DTCN are termed as  $ep_{rn}$ ,  $ep_{vg}$ ,  $ep_{dn}$  and  $ep_{dtn}$ . Consequently, the rate of hidden neurons of ResNet152, VGG19, DenseNet161, and DTCN are termed as  $hn_{rn}$ ,  $hn_{vg}$ ,  $hn_{dn}$ ,  $hn_{dtn}$ , which are tuned through the MUCOA algorithm model. Further, the accuracy and precision are depicted in Eqs (17 & 18).

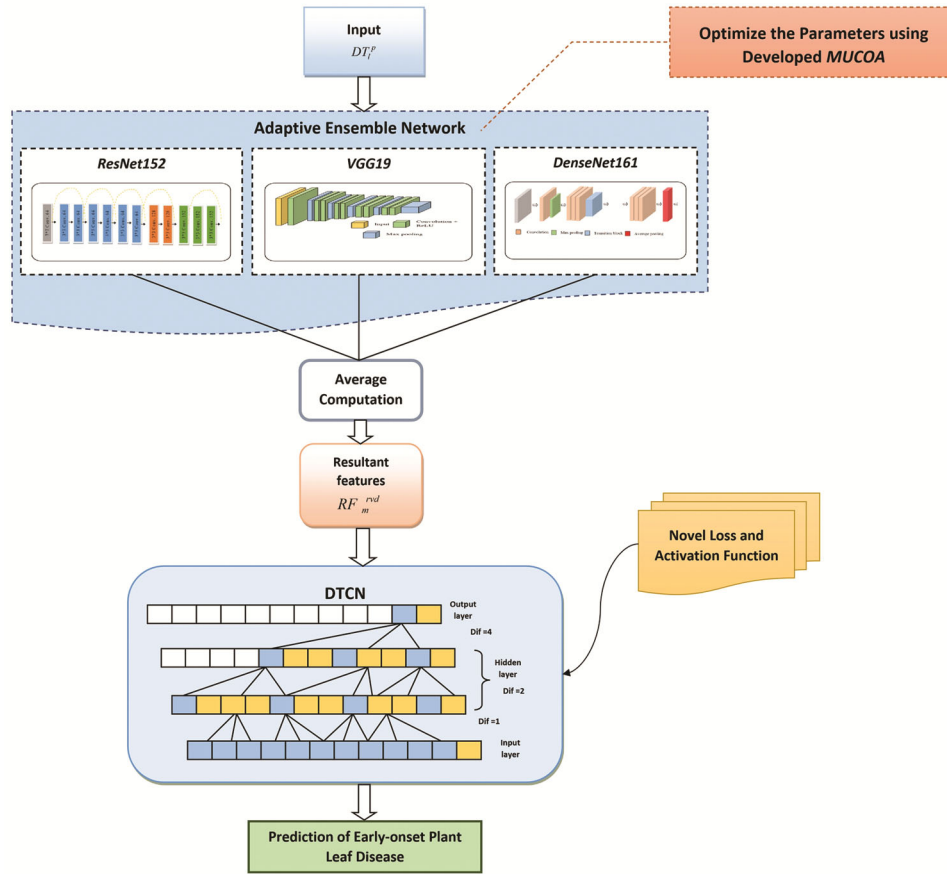


Fig. 4 — Representation of the newly designed AEN-MUCOA model

Accuracy: This metric indicates the proportion of true results (both true positives and true negatives) and is expressed in Eq. (17).

$$acc = \frac{(TP + TN)}{(TP + TN + FP + FN)} \quad \dots (17)$$

(a) Precision: It measures how many of the model's positive predictions are correct. It is represented in Eq. (18).

$$prm = \frac{TP}{TP + FP} \quad \dots (18)$$

Some significant metrics used to calculate the performance of the proposed model are outlined as follows.

(a) Sensitivity: Also known as recall, sensitivity measures the proportion of true positives over all actual positive cases. It is given in Eq. (19).

$$sy = \frac{TP}{TP + FN} \quad \dots (19)$$

(b) Specificity: Specificity measures the proportion of true negatives among all actual negative cases. It is represented in Eq. (20).

$$sp = \frac{TN}{TN + FP} \quad \dots (20)$$

Here, the numbers of true positives, true negatives, false positives, and false negatives are denoted by TP, TN, FP, and FN, respectively.

**Experimental Setup for the Proposed Model**

Experiments on the proposed approach were conducted in Python using Tensor Flow and Keras libraries. Performance analysis was performed using k-fold cross-validation from k = 1 to 5, where the dataset was split into five equal folds. In each iteration, one fold was utilized as the test set and the remaining folds were used for training. For Dataset 1, with a total of 61,486 images, 49,189 images were utilized for training and the remaining 12,297 images were used for testing at each fold. For Dataset 2, which contains 220,592 images, 176,474 images were utilized for training and 44,118 images were utilized for testing at each fold. The performance of the proposed prediction model was evaluated at each fold, and the final performance metrics were averaged across all folds. Additionally, a comparative analysis

of the recommended framework with baseline models was performed.

**Results and Discussion**

**Convergence Analysis**

The convergence behavior of the AEN model with MUCOA compared to the existing COA model is illustrated in Fig. 5. The AEN-MUCOA demonstrates significantly faster convergence, minimizing the cost function in less iteration, which indicates improved computational efficiency. Additionally, it achieves a lower final cost value, leading to more accurate predictions. The AEN-MUCOA model also exhibits greater stability by avoiding local minima and fluctuations in the cost function. This stability is crucial for enhancing reliable predictions for early plant disease using leaf images across diverse datasets.

**Evaluation of the Proposed Model’s Performance by k-Fold Cross-Validation**

The proposed framework is evaluated using k-fold Cross-validation (CV) on both Dataset-1 and Dataset-2, with k rates from 1 to 5. As shown in Fig. 6, performance metrics including accuracy, sensitivity,

and specificity consistently improve as “k” increases. The highest values for all metrics are achieved at k = 5, with Dataset-1 showing accuracy of 94.09%, sensitivity of 94.07%, and specificity of 94.09%, while Dataset-2 achieves accuracy of 94.44%, sensitivity of 94.43%, and specificity of 94.44%.

Notably, the model demonstrates low variance across folds, ensuring consistent performance even with different subsets of data. Additionally, the model’s ability to balance sensitivity and specificity across both datasets reflects its robustness in handling both false positives and false negatives effectively. These results indicate that the AEN-MUCOA performs best with a 5-fold CV, demonstrating strong generalization and stability across both datasets.

**Overall Analysis on Earlier Onset Plant Disease Prediction Model**

The AEN model with MUCOA optimization achieves higher accuracy than all other models across both datasets, as shown in Fig. 7. In Dataset 1, AEN-MUCOA outperforms ResNet152, VGG19, DenseNet161, DTCN, and the proposed AEN with existing COA by 8.04%, 6.31%, 4.55%, 2.76%, and 1.85%, respectively. For Dataset 2, it shows

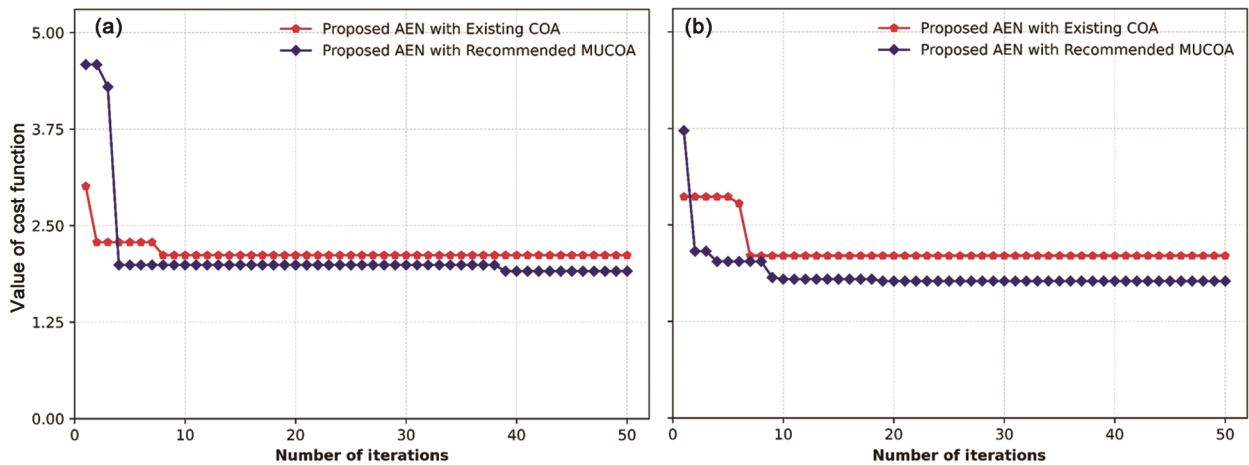


Fig. 5 — Convergence Analysis of the proposed prediction framework for: (a) Dataset 1, (b) Dataset 2

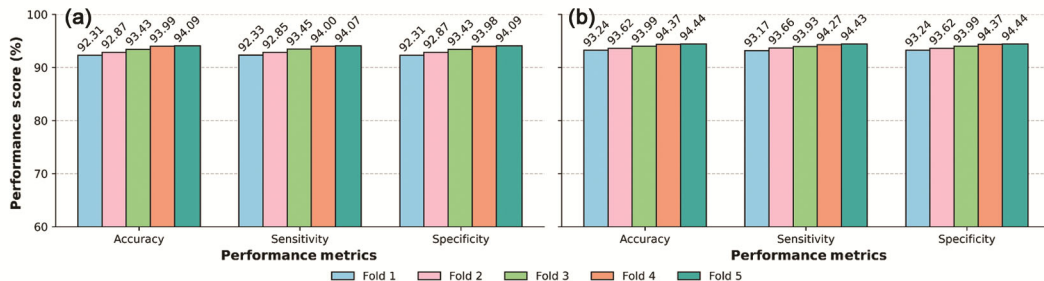


Fig. 6 — Performance analysis of the proposed prediction framework in terms of k-fold CV for: (a) Dataset 1, (b) Dataset 2

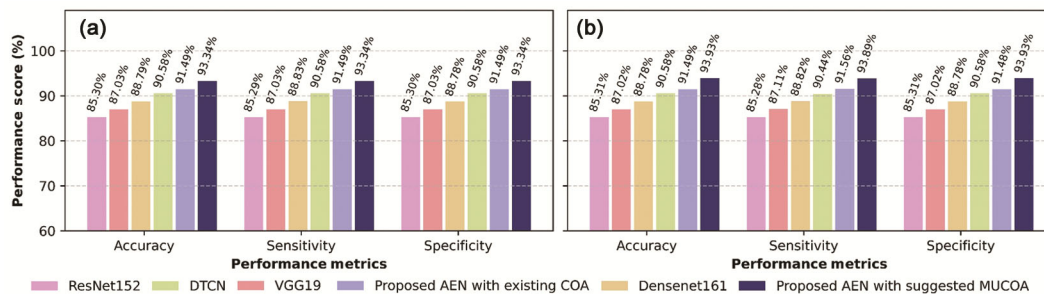


Fig. 7 — Overall performance analysis of the proposed prediction framework with baseline models for: (a) Dataset 1, (b) Dataset 2

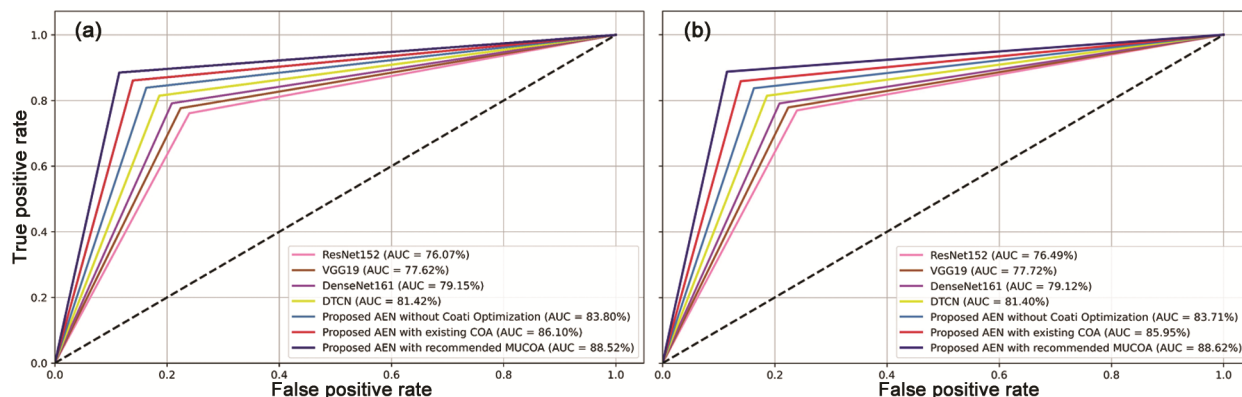


Fig. 8 — ROC and AUC analysis of the suggested prediction framework with various baseline models for: (a) Dataset 1, (b) Dataset 2

improvements of 8.62%, 6.91%, 5.15%, 3.35%, and 2.44% over these baseline models.

These results represent averages across all folds in a 5-fold cross-validation (CV), where AEN-MUCOA consistently achieves optimal performance. In addition to enhancing accuracy, AEN-MUCOA improves true positive predictions while reducing false negatives and false positives, as demonstrated by its superior sensitivity and specificity in Fig. 7.

#### ROC and AUC Analysis of the Designed Approach with Diverse Methods

The ROC curve and AUC are essential metrics for evaluating predictive models. For Dataset 1, the prediction framework achieved an AUC of 88.52%, significantly outperforming baseline models, as shown in Fig. 8(a). In Dataset 2, the model achieved an AUC of 88.62%, further validating its robustness across datasets, as illustrated in Fig. 8(b). These high AUC values highlight the model's superior predictive accuracy, establishing it as a highly effective approach for early-onset plant leaf disease prediction compared to baseline models.

#### Discussion

The designed MUCOA-optimized AEN model integrates ResNet152, VGG19, and DenseNet161,

achieving high accuracy, sensitivity, and specificity. By combining the strengths of these architectures, the ensemble effectively captures both low-level and high-level features, enabling it to identify subtle variations in plant health for early and accurate diagnosis. It helps to effectively ensure robust generalization across various disease classes. This study presents high sensitivity, which reduces false negatives by accurately predicting early-onset diseased leaves, ensuring timely prediction. It also achieves high specificity, minimizing false positives by correctly identifying healthy leaves and preventing unnecessary interventions. These capabilities provide farmers with precise and actionable insights, facilitating targeted interventions to reduce crop losses and improve productivity. Based on the proposed work, recommendations for farmers and a discussion of the challenges and limitations of the framework are outlined as follows:

#### Farmer-Centric Recommendations

The suggested framework's precise disease prediction capability makes it an essential tool for modern agriculture. Farmers can leverage the model's predictions to select suitable pesticides and take preventive measures, improving productivity and

contributing to food security. Moreover, the model aids in preventing the spread of disease within crops, reducing potential losses. The suggested model provides prediction of early-onset disease of plant leaves which enables targeted treatment plans, which can boost food production and promote sustainable farming practices. Farmers can optimize their use of pesticides and fertilizers based on the specific disease identified, enhancing efficiency and sustainability in agriculture.

### Challenges and Limitations

While the recommended model shows promising results, certain limitations must be addressed for real-world deployment. Its performance may degrade when analyzing low-quality or poor-resolution images, which are common in field conditions. Additionally, the model's ability to focus on early-onset diseases in fruits and vegetables, as well as environmental factors, remains limited to key elements, such as soil quality, and pest interactions. To address these limitations, future work will explore the integration of hybrid deep learning frameworks to maximize predictive capabilities. Expanding the dataset to include visual data from various plant fruits and vegetables across diverse agricultural environments will also improve the approach and enabling it to make significant predictions of early-onset disease in all types of plants.

### Conclusions

In the present research, an effective early-onset plant disease prediction model was developed using plant leaf imagery data. Phenotypic images, including both healthy and disease-affected leaves, were obtained from standard repositories and directly used for feature extraction. Relevant features were extracted using the proposed AEN, which combined novel loss and activation functions. The AEN incorporated three standard techniques, namely ResNet152, VGG19, and DenseNet161, and the output features from these networks were averaged to obtain the final feature set. Network parameters were optimized using the MUCOA to improve overall functionality. The extracted features were then processed by the DTCN framework to predict the presence of early-onset diseases in plant leaves. Results demonstrated that the suggested framework outperformed competing benchmark model's sensitivity and specificity, providing reliable predictions of disease onset at an earlier stage.

Experimental findings confirmed the framework's robustness and efficiency in addressing the challenges of plant disease prediction. Future work will aim to extend this approach by incorporating visual imagery of other plant parts, such as fruits and vegetables, and considering ecological factors for a more comprehensive analysis of early disease onset.

### References

- 1 Gayathridevi K, Balasubramanian K, Senthilkumar C & Ramya K, Accurate prediction and classification of corn leaf disease using adaptive moment estimation optimizer in deep learning networks, *J Electr Eng Technol*, **18** (2023) 637–649, <https://doi.org/10.1007/s42835-022-01205-0>.
- 2 Keceli A S, Kaya A, Catal C & Tekinerdogan B, Deep learning-based multi-task prediction system for plant disease and species detection, *Ecol Inf*, **69** (2022) 101679, <https://doi.org/10.1016/j.ecoinf.2022.101679>.
- 3 Singh R N, Krishnan P, Bharadwaj C & Das B, Improving prediction of chickpea wilt severity using machine learning coupled with model combination techniques under field conditions, *Ecol Inf*, **73** (2023) 101933, <https://doi.org/10.1016/j.ecoinf.2022.101933>.
- 4 Islam M M, Adil M A A, Talukder M A, Ahamed M K U, Uddin M A, Hasan M K, Sharmin S, Rahman M M & Debnath S K, Deepcrop: Deep learning-based crop disease prediction with web application, *J Agric Food Res*, **14** (2023) 100764, <https://doi.org/10.1016/j.jafr.2023.100764>.
- 5 Mahlein A K, Plant disease detection by imaging sensors - parallels and specific demands for precision agriculture and plant phenotyping, *APS Publications*, **100(2)** (2016) 241–251, <https://doi.org/10.1094/PDIS-03-15-0340-FE>.
- 6 Ilyas T, Jin H, Siddique M I, Lee S J, Kim H & Chua L, DIANA: A deep learning-based paprika plant disease and pest phenotyping system with disease severity analysis, *Front Plant Sci*, **13(983625)** (2022) 983625, <https://doi.org/10.3389/fpls.2022.983625>.
- 7 Mutka A M, Fentress S J, Sher J W, Berry J C, Pretz C, Nusinow D A & Bart R, Quantitative, image-based phenotyping methods provide insight into spatial and temporal dimensions of plant disease, *Plant Physiol*, **172(2)** (2016) 650–660, <https://doi.org/10.1104/pp.16.00984>.
- 8 Pal T, Jaiswal V & Chauhan R S, DRPPP: A machine learning based tool for prediction of disease resistance proteins in plants, *Comput Biol Med*, **78** (2016) 42–48, <https://doi.org/10.1016/j.compbiomed.2016.09.008>.
- 9 Delnevo G, Girau R, Ceccarini C & Prandi C, A Deep learning and social iot approach for plants disease prediction toward a sustainable agriculture, *IEEE Internet Things J*, **9(10)** (2022) 7243–7250, <https://doi.org/10.1109/JIOT.2021.3097379>.
- 10 Patle K S, Saini R, Kumar A & Palaparthi V S, Field evaluation of smart sensor system for plant disease prediction using lstm network, *IEEE Sens J*, **22(4)** (2022) 3715–3725, <https://doi.org/10.1109/JSEN.2021.3139988>.
- 11 Shivling V D, Ghanshyam C, Kumar R, Kumar S, Sharma R, Kumar D, Sharma A & Sharma S K, Prediction model for predicting powdery mildew using ann for medicinal plant—picrorhizakurrooa, *J Inst Eng India Ser B*, **98** (2017) 77–81, <https://doi.org/10.1007/s40031-016-0225-9>.

- 12 Ashwini C & Sellam V, EOS-3D-DCNN: Ebola optimization search-based 3D-dense convolutional neural network for corn leaf disease prediction, *Neural Comput Appl*, **35** (2023) 11125–11139, <https://doi.org/10.1007/s00521-023-08289-3>.
- 13 Stephen A, Punitha A & Chandrasekar A, Optimal deep generative adversarial network and convolutional neural network for rice leaf disease prediction, *Visual Comput*, **40** (2024) 919–936, <https://doi.org/10.1007/s00371-023-02823-z>.
- 14 Sankarshwaran S P, Jayaraman G, Muthukumar P & Krishnan A S, Optimizing rice plant disease detection with crossover boosted artificial hummingbird algorithm based AX-RetinaNet, *Environ Monit Assess*, **195**(9) (2023) 1070, <https://doi.org/10.1007/s10661-023-11612-z>.
- 15 Liu G, Peng J & Latif A A A E, SK-MobileNet: A lightweight adaptive network based on complex deep transfer learning for plant disease recognition, *Arabian J Sci Eng*, **48** (2023) 1661–1675, <https://doi.org/10.1007/s13369-022-06987-z>.
- 16 Tanwar S & Singh J, ResNext50 based convolution neural network-long short term memory model for plant disease classification, *Multimedia Tools Appl*, **82** (2023) 29527–29545, <https://doi.org/10.1007/s11042-023-14851-x>.
- 17 Khanna M, Singh L K, Thawkar S & Goyal M, PlaNet: a robust deep convolutional neural network model for plant leaves disease recognition, *Multimedia Tools Appl*, **83** (2024) 4456–4517, <https://doi.org/10.1007/s11042-023-15809-9>.
- 18 Cardellicchio A, Solimani F, Dimauro G, Petrozza A, Summerer S, Cellini F & Reno V, Detection of tomato plant phenotyping traits using YOLOv5-based single stage detectors, *Comput Electron Agric*, **207** (2023) 107757, <https://doi.org/10.1016/j.compag.2023.107757>.
- 19 Bhatia A, Chug A, Singh A P & Singh D, Fractional mega trend diffusion function-based feature extraction for plant disease prediction, *Int J Mach Learn Cybern*, **14** (2023) 187–212, <https://doi.org/10.1007/s13042-022-01562-2>.
- 20 Arshad F, Mateen M, Hayat S, Wardah M, Al-Huda Z, Gu Y H & Al-antari M A, PLDPNet: End-to-end hybrid deep learning framework for potato leaf disease prediction, *Alexandria Eng J*, **78** (2023) 406–418, <https://doi.org/10.1016/j.aej.2023.07.076>.
- 21 Yang B, Wang Z, Guo J, Guo L, Liang Q, Zeng Q, Zhao R, Wang J & Li C, Identifying plant disease and severity from leaves: A deep multitask learning framework using triple-branch Swin Transformer and deep supervision, *Comput Electron Agric*, **209** (2023) 107809, <https://doi.org/10.1016/j.compag.2023.107809>.
- 22 Dahiya S, Gulati T & Gupta D, Performance analysis of deep learning architectures for plant leaves disease detection, *Meas Sens*, **24** (2022) 100581, <https://doi.org/10.1016/j.measen.2022.100581>.
- 23 Bhakta I, Phadikar S, Majumder K, Mukherjee H & Sau A, A novel plant disease prediction model based on thermal images using modified deep convolutional neural network, *Precis Agric*, **234** (2023) 23–39, <https://doi.org/10.1007/s11119-022-09927-x>.
- 24 Chug A, Bhatia A, Singh A P & Singh D, A novel framework for image-based plant disease detection using hybrid deep learning approach, *Soft Comput*, **27** (2023) 13613–13638, <https://doi.org/10.1007/s00500-022-07177-7>.
- 25 Ramanadham K L & Savarimuthu N, vCrop: an automated plant disease prediction using deep ensemble framework using real field images, *Sadhana*, **47**(4) (2022) 268, <https://doi.org/10.1007/s12046-022-02041-8>.
- 26 Dehghani M, Montazeri Z, Trojovska E & Trojovsky P, Coati optimization algorithm: A new bio-inspired metaheuristic algorithm for solving optimization problems, *Knowledge-Based Syst*, **259** (2023) 110011, <https://doi.org/10.1016/j.knsys.2022.110011>.
- 27 Alam T S, Jowthi C B & Pathak A, Comparing pre-trained models for efficient leaf disease detection: a study on custom CNN, *J Electr Syst Inf Technol*, **11**(1) (2024) 12, <https://doi.org/10.1186/s43067-024-00137-1>.
- 28 Nguyen T H, Nguyen T N & Ngo B V, A VGG-19 Model with Transfer Learning and Image Segmentation for Classification of Tomato Leaf Disease, *Agric Eng*, **4**(4) (2022) 871–887, <https://doi.org/10.3390/agriengineering4040056>.
- 29 Too E C, Yujian L, Kwao P, Njukia S, Mosomic M E & Kibet J, Deep pruned nets for efficient image-based plants disease classification, *J Intell Fuzzy Syst*, **37**(3) (2019) 4003–4019, <https://doi.org/10.3233/JIFS-190184>.
- 30 Wan R, Mei S, Wang J, Liu M & Yang F, Multivariate temporal convolutional network: A deep neural networks approach for multivariate time series forecasting, *Electron*, **8**(8) (2019) 876 <https://doi.org/10.3390/electronics8080876>.